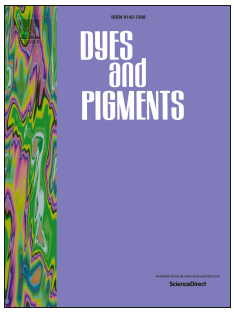


# An ESIPT coupled AIE fluorescent probe for biothiols detection and imaging based on a chalcone fluorophore

Fangfang Dai, Min Zhao, Fangzhou Yang, Tingting Wang, Chao Wang

PII: S0143-7208(20)31324-3

DOI: https://doi.org/10.1016/j.dyepig.2020.108627

Reference: DYPI 108627

To appear in: *Dyes and Pigments*

Received Date: 22 March 2020

Revised Date: 3 June 2020

Accepted Date: 3 June 2020

Please cite this article as: Dai F, Zhao M, Yang F, Wang T, Wang C, An ESIPT coupled AIE fluorescent probe for biothiols detection and imaging based on a chalcone fluorophore, *Dyes and Pigments*, https://doi.org/10.1016/j.dyepig.2020.108627.

**Author Statement**

**Dai Fangfang:** Methodology, Investigation, Writing- Original draft. **Zhao Min:** Investigation, Writing- Original draft. **Yang Fangzhou:** Investigation, **Wang Tingting:** Investigation, **Wang Chao:** Conceptualization, Writing - Review & Editing, Supervision, Funding acquisition.

## Graphical abstract

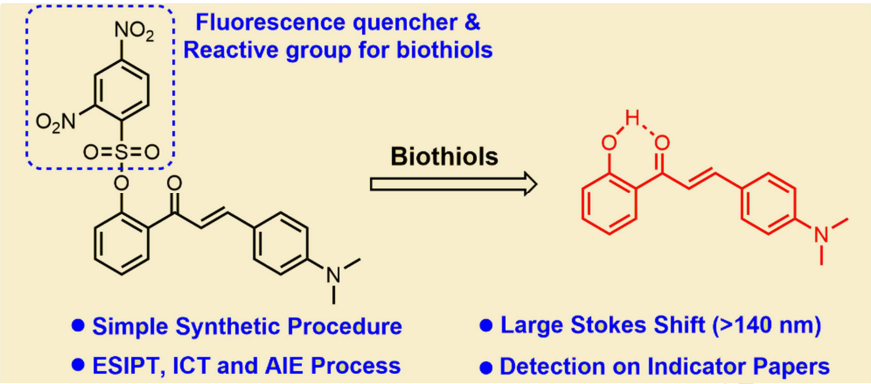

# An ESIPT coupled AIE fluorescent probe for biothiols detection and imaging based on a chalcone fluorophore

Fangfang Dai, Min Zhao, Fangzhou Yang, Tingting Wang, Chao Wang*

College of Chemistry and Chemical Engineering, Shaanxi Key Laboratory of Chemical Additives for Industry, Shaanxi University of Science and Technology, Xi'an 710021, China

*Corresponding author.

E-mail address: wangchao@sust.edu.cn (C. Wang)

**Abstract:**

Biothiols are closely related to numerous physiological and pathological processes in living organisms and cells. Fluorescent probes are powerful tools for sensitive detection and imaging of biothiols in biological samples. In this work, we developed a novel turn-on fluorescent probe **DNBS-HCA** for biothiols detection based on the simple 2′-Hydroxychalcone (**HCA**) fluorophore, which possesses an excited-state intramolecular proton transfer (ESIPT) coupled aggregation-induced emission (AIE) characteristic. The 2′-hydroxyl group of **HCA** fluorophore is caged with a biothiols reactive 2,4-dinitrobenzenesulfonyl (DNBS) moiety, which blocks the ESIPT process and quenches the fluorescence. The reaction between probe and biothiols will produce the **HCA** fluorophore with large Stokes shift and long-wavelength red fluorescence emission. The biothiols in solutions and living cells can be conveniently detected with the probe **DNBS-HCA** due to its excellent properties such as simple synthetic procedure, remarkable fluorescence enhancement, good sensitivity, high selectivity and low cytotoxicity. Benefiting from the AIE characteristic, the probe is also applied for biothiols detection on indicator papers with RGB color red values, which can be handily obtained by smartphone app.

**Keywords:**

Fluorescent probe; Biothiols; Aggregation induced emission; ESIPT; Chalcone

## 1. Introduction

Biological thiol compounds (biothiols), such as glutathione (GSH), Cysteine (Cys) and Homocystine (Hcy), are closely related to numerous physiological and pathological processes in living organisms and cells. Due to the redox properties of the thiol groups, these biothiols play crucial roles in intracellular redox homeostasis, detoxification, proteins folding, activity regulation of enzymes, cellular signal transduction, and gene expression, *etc* [1, 2]. Abnormal concentrations of these biothiols have been reported to associate with some disease processes such as cancer, inflammation, cardiovascular diseases, and neurodegenerative diseases [3-5]. Owing to the significance of these biothiols for living organisms, the detection of these biothiols is of great importance for the understanding of the biological functions, also for the diagnosis and treatment of related diseases.

Fluorescent probes are powerful tools for sensitive detection of biothiols in biological samples. Various different kinds of organic fluorophores have been employed for fluorescent sensing and imaging of intracellular biothiols with high temporal-spatial resolution [6-13]. However, most of the ordinary fluorescent probes for biothiols detection show aggregation-caused quenching (ACQ) effect and quenched fluorescence in aqueous biological samples. In contrast, some novel fluorophores (e.g., tetraphenylethene and hexaphenylsilole) with the aggregation induced emission (AIE) characteristic have been reported to overcome this defect [14-16]. These AIE fluorophores reveal good features such as higher brightness, lower background noise and better photostability, which are beneficial for fluorescent

imaging of biothiols in living cells [17-24].

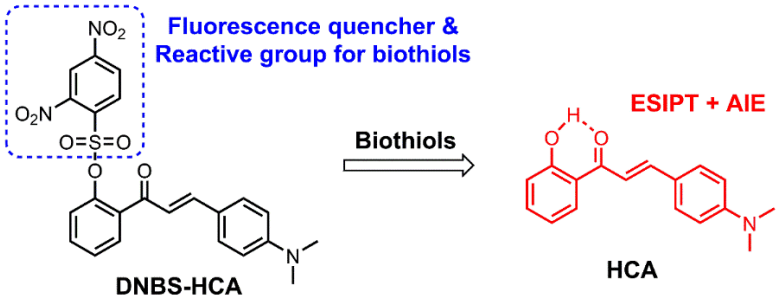


**Scheme 1.** The mechanism of the probe **DNBS-HCA** response to biothiols.

Herein, we design and synthesis a novel turn-on fluorescent probe **DNBS-HCA** for biothiols detection and imaging based on a simple 2′-Hydroxychalcone (**HCA**) fluorophore caged by a 2,4-dinitrobenzenesulfonyl (DNBS) moiety acting as biothiols-reactive fluorescence quencher (Scheme 1). The N, N-dimethylamino unit and 2'-hydroxyacetophenone unit in the **HCA** fluorophore are respectively regarded as electron donor and acceptor (D-A) of the intramolecular charge transfer (ICT) process [25]. The **HCA** fluorophore also possesses an excited-state intramolecular proton transfer (ESIPT) coupled AIE characteristic [26-34]. All these processes produce the large Stokes shift (>140 nm) and red shift of fluorescence wavelength.

The fluorescence property of the probe **DNBS-HCA** is totally different from the **HCA** fluorophore. The DNBS moiety introduced to cage the 2′-hydroxyl group of **HCA** fluorophore can quench the fluorescence through the photo-induced electron transfer (PET) effect. Moreover, the ESIPT process is also blocked when the hydroxyl group in 2'-hydroxyacetophenone unit is caged [26, 35, 36]. The reaction between probe **DNBS-HCA** and biothiols will produce a 2,4-dinitrothiophenolate (DNTP) and the **HCA** product, which gives rise to a turn-on red fluorescence (Scheme 1 and Fig.

S1). This reaction mechanism between 2,4-dinitrobenzenesulfonate ester and biothiols has been verified by many reports [37-48]. The AIE characteristic of the **HCA** product promises a remarkable fluorescence enhancement and the feasibility for biothiols detection in the solid-phase on indicator papers.

## 2. Experimental section

### *2.1. Reagents and general methods*

All chemical reagents were purchased from commercial companies and used without further purification. The NMR spectra were carried out on a 400 MHz Bruker ADVANCE III spectrometer. Mass spectrum was carried out on a Thermo Scientific LTQ Orbitrap XL FTMS. HPLC test was carried out on a Waters HPLC-1525. The UV-*vis* absorption spectra were measured by using an Agilent Cary 60 spectrometer. Fluorescence spectra were recorded on a ThermoFisher Scientific Lumina fluorescence spectrometer. Fluorescent imaging of living cells was performed on a Carl Zeiss LSM800 Confocal Laser Scanning Microscope (CLSM).

### *2.2. Synthesis of **DNBS-HCA***

The 2′-hydroxychalcone (**HCA**) was easily synthesized by a simple one-step condensation reaction according to the reported method [49]. A 2'-hydroxyacetophenone (4.087 g, 0.03 mol) and 4-dimethylaminobenzaldehyde (4.467 g, 0.03 mol) were added to a 250 mL round-bottom flask and dissolved by adding ethanol (50 mL). Then, the KOH (4.208 g, 0.075 mol) was added. The reaction mixture was reflux at 60 °C for 12 h. After the solution was cooled, 3 M HCl was added to adjust the pH to 6. The solid precipitation was filtered out and the residual

solvent was removed under reduced pressure. The crude product was purified through silica gel column chromatographic (PE:EtOAc=10:1 as eluent). A red pure solid product was obtained (6.30 g, 78%). $^{1}$H NMR (400 MHz, Chloroform-d): δ 13.26 (s, 1H), 7.95 (dd, *J* = 8.3, 6.9 Hz, 2H), 7.61 (d, *J* = 8.9 Hz, 2H), 7.52-7.46 (m, 2H), 7.04 (dd, *J* = 8.3, 0.8 Hz, 1H), 6.97-6.92 (m, 1H), 6.73 (d, *J* = 8.9 Hz, 2H), 3.09 (s, 6H).

The **HCA** (91.5 mg, 0.34 mmol) was added to a 100 mL round bottom flask and dissolved in 7 mL $CH_2Cl_2$. $Et_3N$ (100 μL) was added to the reaction in an ice bath, stirred at 0 °C for 30 min. Then, 2,4-dinitrobenzenesulfonyl chloride (183.5 mg, 0.68 mmol) was added, and the reaction was conducted at room temperature for 8 h. The solvent was removed under reduced pressure. The crude product was purified by silica gel column chromatography (PE:EtOAc=5:1 as eluent). A brown solid product **DNBS-HCA** was obtained (110 mg, 64%). $^{1}$H NMR (400 MHz, Chloroform-d): δ 8.34-8.29 (m, 2H), 8.19-8.13 (m, 1H), 7.68-7.58 (m, 2H), 7.54-7.45 (m, 2H), 7.26-7.16 (m, 3H), 6.71 (d, *J* = 15.6 Hz, 1H), 6.59 (d, *J* = 8.8 Hz, 2H), 3.08 (s, 6H). $^{13}$C NMR (100 MHz, DMSO-d6) δ 189.52, 152.64, 151.32, 148.29, 146.87, 145.93, 134.51, 133.75, 133.06, 131.85, 131.16, 130.86, 128.90, 127.92, 123.69, 121.37, 121.22, 120.01, 112.15, 39.91. HRMS (ESI) m/z: calcd $[M+H]^+$ for $C_{23}H_{20}N_3O_8S$ 498.0971, found 498.0959.

*2.3. Spectra properties of **DNBS-HCA***

The stock solutions of **DNBS-HCA** (10 mM) and **HCA** (10 mM) were prepared in DMSO. The test solutions of **DNBS-HCA** (40 μM) and **HCA** (40 μM) were prepared by diluting the stock solution with DMSO-HEPES buffer (v/v = 3:7, 50 mM, pH =

7.4).

The absorption and fluorescence spectra of **DNBS-HCA** with or without different biothiols (400 μM, 10 equiv) were measured. The fluorescence response of **DNBS-HCA** with different concentration of biothiols were recorded after incubating with these biothiols for 60 min at room temperature.

The probe **DNBS-HCA** with excess Cys was prepared in MeOH/$H_2O$ (v/v = 5/5) solution for HPLC and mass spectra test. The sample used for $^1$H NMR test was prepared in DMSO/$H_2O$ (v/v = 3/7) solution and extracted with the ethyl acetate. The extract from ethyl acetate phase was dissolved in deuterium DMSO and used for $^1$H NMR test.

The limits of detection (LOD) for different biothiols were determined by using the 3δ/k, where δ is the standard deviation (SD) of the blank sample solution without any biothiols and k is the slope of the fitted curve of fluorescence intensity with biothiols concentration. The time-dependent fluorescence responses of **DNBS-HCA** were recorded with the addition of excess biothiols (400 μM, 10 equiv).

The selectivity of **DNBS-HCA** for biothiols (Cys, GSH and Hcy) was evaluated by the fluorescence response with the addition of excess biological species (400 μM, 10 equiv) including different amino acids (Gly, Tyr, Leu, Gln, Glu, Arg, Thr, Lys), metal ions ($K^+$, $Na^+$, $Mg^{2+}$, $Cu^{2+}$, $Fe^{2+}$), and protein BSA (1 mg/mL). The biothiols (400 μM) pretreated with equivalent thiol scavenger N-ethyl-maleimide (NEM, 400 μM) were also detected.

*2.4. Detection of biothiols on indicator papers*

The indicator papers of probe **DNBS-HCA** for biothiols detection were prepared with filter papers (φ=0.5 cm) by immersing into solution of **DNBS-HCA** (1 mM) dissolved in acetonitrile and then drying in atmosphere. The solutions (10 μL) of biothiols with different concentrations in DMSO-HEPES buffer (v/v = 3:7, 50 mM, pH = 7.4) were dropped to the indicator papers and incubated for 30 min. The photograph of the fluorescence on the indicator papers was taken by a smartphone camera under a 365 nm UV light. The relative intensities of the red fluorescence were quantified with the red values of RGB color obtained by a smartphone application (Color recognizer) as the previous report [50].

*2.5. Cell culture and fluorescent imaging*

Human prostate cancer PC3 cells and human lung adenocarcinoma A549 cells were maintained in a $CO_2$ incubator (ESCO) at 37°C with humidified atmosphere of 5% $CO_2$. The cells were cultured and prepared for fluorescent imaging as previous described [51], which were cultured in Dulbecco's Modified Eagle's Medium (DMEM, Hyclone) supplemented with 10% fetal bovine serum (FBS, Gibco), penicillin (100 U/mL) and streptomycin (100 μg/mL). The cells used for fluorescent imaging were cultured in glass-bottom dishes (φ=20 mm) for 24 h, and then treated with or without 0.5 mM thiol scavenger NEM in PBS for 30 min at 37°C. After washed with PBS (3×1 mL), the cells were stained with **DNBS-HCA** (10 μM in PBS) at 37°C for 30 min. The cells were then washed with PBS (3×1 mL) and imaged using the CLSM with a ×63 objective lens. The excitation wavelength was 488 nm. The emission wavelength was 560-700 nm for red channel and 500-560 nm for green

channel. The average fluorescent intensity in fluorescent imaging was measured by the software Image J.

*2.6. Cytotoxicity of **DNBS-HCA***

The cell counting kit-8 (CCK-8, Beyotime Biotechnology) was used to assess the cytotoxicity of **DNBS-HCA**. The A549 cells were seeded on 96-well cell culture plates ($3\times10^3$ cells/well, 100 μL) and cultured for 24 h. Then the probe **DNBS-HCA** dissolved in 10 μL medium was added into the wells with the final concentration from 0 to 16 μM and incubated for 24 h. The CCK-8 solution (10 μL) was then added and incubated for 1 h. The optical density (OD) at 450 nm was recorded by a multimode microplate reader (Varioskan Flash, Thermo Scientific). The cell viabilities were obtained from the $OD_{450\ nm}$ ratio between **DNBS-HCA** treated groups and control group.

## 3. Results and discussion

*3.1. Design and synthesis of the probe **DNBS-HCA***

The synthetic procedure of **DNBS-HCA** is very simple and convenient (Scheme 2). The **HCA** fluorophore was readily synthesized following the literature method [26, 36, 49] through a simple one-step Claisen-Schmidt condensation reaction between 2'-hydroxyacetophenone and 4-dimethylaminobenzaldehyde with high yield 78%. The probe **DNBS-HCA** was then prepared with the **HCA** fluorophore and 2,4-dinitrobenzenesulfonyl chloride in 64% yield. The structure of **DNBS-HCA** was characterized by $^1$H NMR, $^{13}$C NMR, and HRMS (Fig. S2).

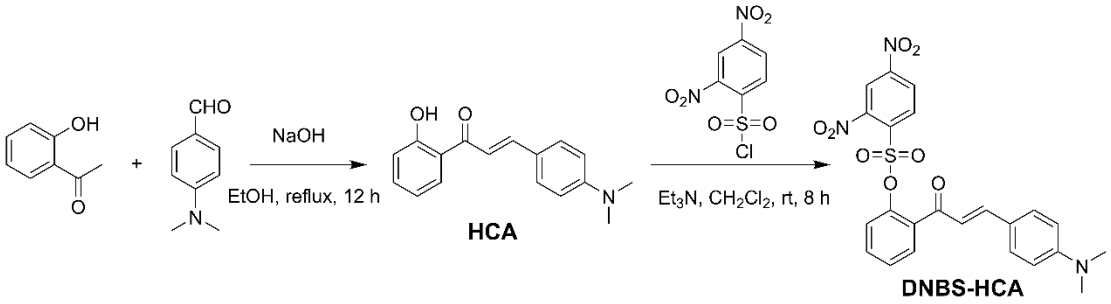


**Scheme 2.** Synthetic route of the probe **DNBS-HCA**.

*3.2. Spectra properties of the **HCA** fluorophore*

**HCA** fluorophore is the prospective product of the reaction between **DNBS-HCA** and biothiols (Scheme 1). It has been reported that the **HCA** fluorophore possesses an ESIPT active AIE phenomenon [26-31]. The fluorescent spectra of this fluorophore in different solvents are shown in Fig. S3. It displays weakly green fluorescence in some organic solvents. In contrast, it exhibits stronger, red fluorescence in the aqueous solution. The mixed solvent system (water/THF) is used to verify the AIE characteristic. The fluorescence shows gradually increased intensity and red-shifted wavelength following the rise of the water content (Fig. S4). The UV-vis absorption spectrum and fluorescence spectrum of **HCA** in mixed DMSO-HEPES buffer (v/v = 3:7, 50 mM, pH = 7.4) are shown in Fig. S5. The AIE property of **HCA** was further performed in mixed DMSO/HEPES buffer. As shown in Fig. S6, the aggregation-induced red emission was enhanced with the increase of water proportion. The mixed DMSO/HEPES buffer (v/v = 3:7, 50 mM, pH = 7.4) is a critical fraction for **HCA** at the concentration of 40 μM. When 100 μM **HCA** was dissolved in this buffer, a significant aggregation-induced red emission will produce. We also confirm the particle size of the aggregated **HCA** fluorophore in HEPES buffer fraction

exceeding 70%. The dynamic light scattering (DLS) test was used to observe the particle size. As shown in Fig. S7, the particle size is increased with the rise of HEPES buffer fraction. The large Stokes shift (about 140 nm) of the **HCA** fluorophore can reduce the self-absorption and quenching, which is remarkable for fluorescence detection and imaging.

The fluorescence property of **HCA** product in different pH solutions were investigated. As shown in Fig. S8, the fluorescent intensity of **HCA** displays good stability in the range of pH 3-9 with 30% DMSO. While in the strong base solution of pH 11, the fluorescence spectrum of **HCA** shows a distinct blue-shift and a decrease of fluorescence intensity.

*3.3. Spectra properties of **DNBS-HCA** for biothiols detection*

The absorption spectra of **DNBS-HCA** for biothiols detection were firstly measured. As shown in Fig. 1a, the probe **DNBS-HCA** displays an absorption peak at 440 nm with a molar extinction coefficient ($\varepsilon = 1.8 \times 10^4\ M^{-1}cm^{-1}$) in DMSO-HEPES buffer (v/v = 3:7, 50 mM, pH = 7.4). After reacting with Cys, the absorption peak reveals a weak red-shift to 460 nm and slightly enhanced intensity with a molar extinction coefficient ($\varepsilon = 2.6 \times 10^4\ M^{-1}cm^{-1}$). Meanwhile, the absorption appears at 300-400 nm after reacting with Cys is attributed to the DNTP product [17]. The **HCA** fluorophore was also brought into the measurement as a control, because it is the expected fluorescence product of reaction between **DNBS-HCA** and biothiols. Indeed, the absorption spectra of **DNBS-HCA** with Cys is exactly similar to that of the **HCA** fluorophore with a molar extinction coefficient ($\varepsilon = 2.8 \times 10^4\ M^{-1}cm^{-1}$). All the

spectral changes are in accord with the predictable mechanism of a 2,4-dinitrobenzenesulfonate ester for biothiols detection (Scheme 1 and Fig. S1). Some other experiments such as $^{1}$H NMR, mass spectra and HPLC were carried out to verify the mechanism and the product (Fig. S9, S10 and S11). The $^{1}$H NMR spectrum of **DNBS-HCA** with excess Cys is totally same as that of **HCA**. The HRMS for **HCA** product $[M+H]^{+}$ was calcd to 268.1338, and found 268.1336. The retention times of chromatograph peak in HPLC directly reveals the produce of **HCA** and the decrease of **DNBS-HCA**. All these results confirm the product is the **HCA** fluorophore.

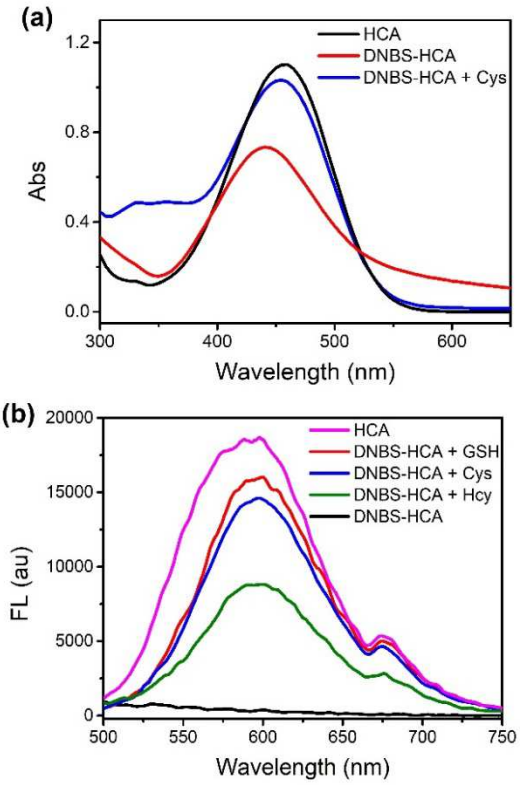


**Fig. 1.** The spectra properties of probe **DNBS-HCA** (40 μM) with or without biothiols. (a) The absorption spectra of **HCA**, **DNBS-HCA** with or without Cys (400 μM). (b) The fluorescence spectra of **HCA**, **DNBS-HCA** with (400 μM) or without different biothiols (GSH, Cys and Hcy).

The fluorescence spectra of **HCA**, **DNBS-HCA** and **DNBS-HCA** with different

biothiols (GSH, Cys and Hcy) are shown in Fig. 1b. The probe **DNBS-HCA** (40 μM) in DMSO-HEPES buffer (v/v = 3:7, 50 mM, pH = 7.4) shows almost no fluorescence, which is attributed to the quench effect of the DNBS moiety. After the addition of excess biothiols (10 eq), a remarkable turn-on fluorescence peak at 600 nm is observed. It implies the remove of the biothiols-reactive DNBS moiety. The emission intensity at 600 nm shows 94-fold, 92-fold and 51-fold enhancement for addition of GSH, Cys and Hcy, respectively. The fluorescence intensity of **DNBS-HCA** with excess GSH is close to that of the **HCA** fluorophore. These results indicate the produce of **HCA** product with a remarkable turn-on fluorescence from reaction between **DNBS-HCA** and biothiols.

*3.4. Quantitative detection of biothiols with **DNBS-HCA***

The quantitative analysis of **DNBS-HCA** for biothiols detection was measured by gradual addition of different biothiols (GSH, Cys or Hcy). As shown in Fig. 2a, the fluorescence spectra reveal significantly and gradually increase with the addition of various amounts of GSH. The fluorescence of **DNBS-HCA** with various amounts of Cys or Hcy reveals a similar trend (Fig. S12). The fluorescence intensity at 600 nm was calculated to clarify the sensitivity of the reaction between **DNBS-HCA** and biothiols. In Fig. 2b, the fluorescence intensity at 600 nm is enhanced continuously with the increase of the biothiols concentration until it reaches a maximum plateau with a few equiv (1-5 equiv) of biothiols.

In the low concentration range of biothiols, the fluorescence intensity at 600 nm shows good linear correlation with the biothiols concentration (Fig. 2c). The linear

correlation coefficient for GSH, Cys and Hcy are 0.977, 0.977 and 0.988, respectively. The limits of detection (LOD) for GSH, Cys and Hcy are determined to be 0.227, 0.283 and 1.826 μM according to the 3δ/slope. These results demonstrate **DNBS-HCA** has good sensitivity for biothiols sensing.

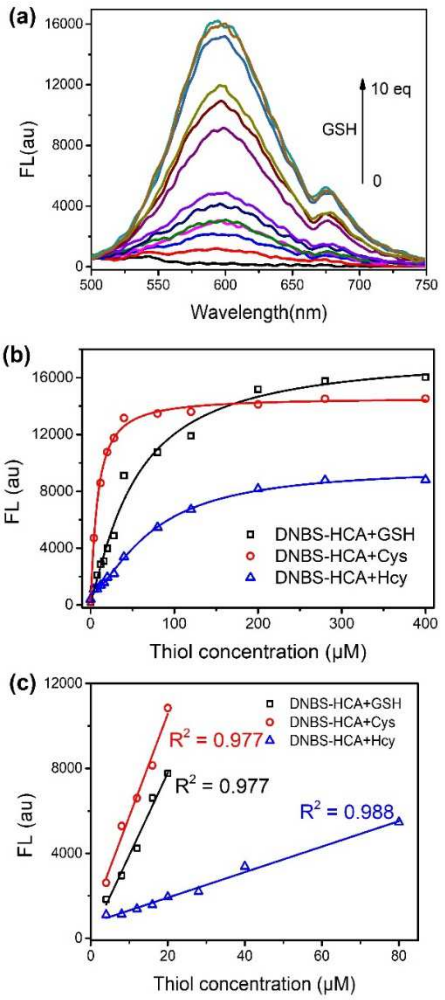


**Fig. 2.** Fluorescence of **DNBS-HCA** (40 μM) upon addition of different concentrations of biothiols (0-400 μM). (a) The fluorescence spectra of **DNBS-HCA** (40 μM) with different concentrations of GSH. (b) The relationship between fluorescence intensity of **DNBS-HCA** at 600 nm and biothiols concentrations. (c) The fluorescence intensity of **DNBS-HCA** at 600 nm as a function of biothiols in the low concentration range.

*3.5. Time-dependent fluorescence responses of **DNBS-HCA** for biothiols*

The time-dependent fluorescence responses of **DNBS-HCA** for biothiols were determined. As shown in Fig. 3a and Fig. S13, the fluorescence band at 600 nm displays gradually increasement with excess biothiols (10 equiv GSH, Cys or Hcy). The fluorescence intensity at 600 nm was also collected to evaluate the response efficiency over time with biothiols. The fluorescence intensity reaches its maximum value in less than 15 minutes (approximately 3 min for Cys, and 15 min for GSH, Hcy). The kinetics process of biothiols response with **DNBS-HCA** reveals the fast reactions between them.

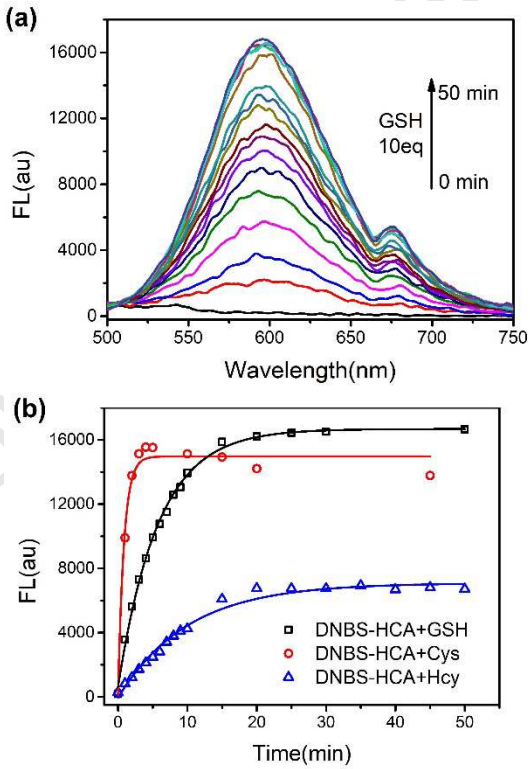


**Fig. 3.** Time-dependent Fluorescence of **DNBS-HCA** (40 μM) upon addition of different biothiols (10 eq). (a) Time-course fluorescence spectra of **DNBS-HCA** (40 μM) with GSH (400 μM, 10 equiv). (b) Fluorescence intensity changes at 600 nm of **DNBS-HCA** (40 μM) in the presence of GSH, Cys, or Hcy (400 μM).

The effect of water volume on the biothiol-sensing kinetics process was evaluated.

The fluorescent intensity at 600 nm was collected to reveal the kinetics process, which was shown in Fig. S14. The results demonstrate that the increase of water volume from 70% to 100% will decrease the reaction rate. The kinetics process of probe **DNBS-HCA** in different pH solutions (with 30% DMSO) was also verified. As shown in Fig. S15, The acidic pH 5 causes the decrease of reaction rate, while the alkaline pH 9 promotes the detect reaction.

*3.6. Selectivity of **DNBS-HCA** for biothiols*

The selectivity of **DNBS-HCA** for biothiols (Cys, GSH, Hcy) was evaluated by comparison with various biological species including amino acids (Gly, Tyr, Leu, Gln, Glu, Arg, Thr, Lys), representative metal ions ($K^+$, $Na^+$, $Mg^{2+}$, $Cu^{2+}$, $Fe^{2+}$) and protein BSA. The fluorescence intensity of **DNBS-HCA** with all these species shows almost no change compared with that of the probe. The remarkable enhancement of the fluorescence intensity with Cys, GSH or Hcy indicates the high selectivity of **DNBS-HCA** for biothiols over these species (Fig. 4). Noteworthily, the fluorescence of **DNBS-HCA** with protein BSA containing some disulfide bonds and free thiol has also no change, indicating the probe **DNBS-HCA** will not react with non-protein thiols.

The selectivity of **DNBS-HCA** for biothiols sensing in solutions was also verified by using the thiol scavenger NEM (Fig. 4). **DNBS-HCA** reveals very weak fluorescence enhancement with Cys and GSH pretreated by equivalent NEM. The thiol of Cys and GSH is almost blocked by the scavenger NEM, which results in the negligible fluorescence changes.

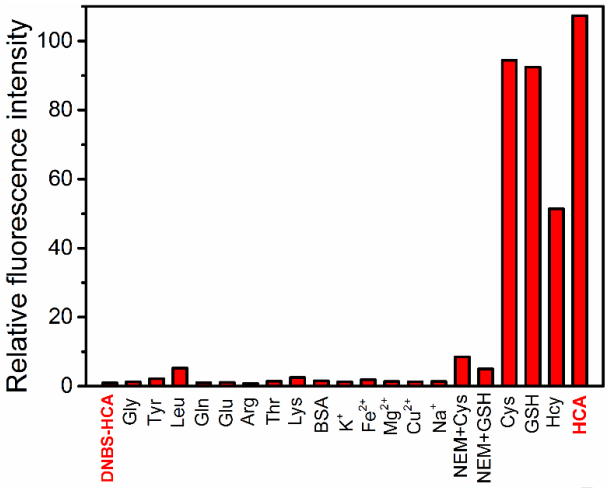


**Fig. 4.** Relative fluorescence intensity of **DNBS-HCA** (40 μM) at 600 nm with different biological species (400 μM, 10 equiv) including amino acids (Gly, Tyr, Leu, Gln, Glu, Arg, Thr, Lys), metal ions ($K^+$, $Na^+$, $Mg^{2+}$, $Cu^{2+}$, $Fe^{2+}$), protein BSA (1 mg/mL), and biothiols (400 μM) pretreated with equivalent NEM.

*3.7. Detection of biothiols on indicator papers with **DNBS-HCA***

In consideration of the AIE characteristic of the **HCA** product from the detection reaction, the availability of the probe **DNBS-HCA** for biothiols detection on indicator papers was carried out. Filter papers deposited with **DNBS-HCA** were used for biothiols detection in solid phase. The solutions of biothiols with different concentrations were dropped onto the indicator papers. The photograph of the turn-on red fluorescence on the indicator papers with the addition of Cys and GSH was taken under 365 nm UV light by a smartphone camera (Fig. 5a and Fig. S16a). The red color of fluorescence on indicator papers shows remarkable enhancement following the increase of biothiols concentration.

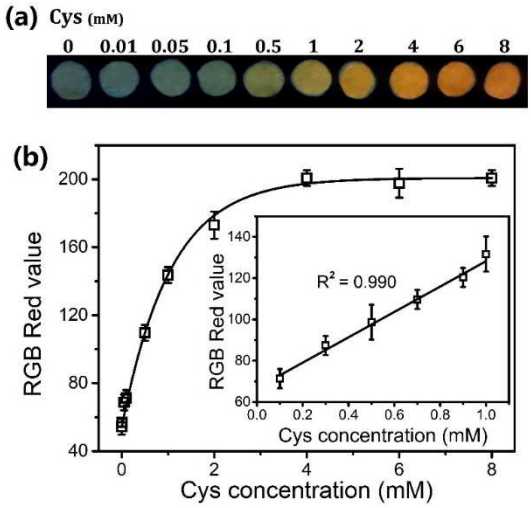


**Fig. 5.** Photograph of fluorescence and intensities on indicator papers with **DNBS-HCA** for Cys detection. (a) Photograph of fluorescence on indicator papers with **DNBS-HCA** for Cys detection. (b) Plot of RGB red values of fluorescence on indicator papers with Cys concentration. Inset: Linear range of RGB red values of fluorescence with Cys concentration.

The relative intensity of the red fluorescence on indicator papers was calculated to obtain the quantitative relation with the concentration of biothiols. The red values of the RGB color in the photographs were also obtained by a convenient smartphone application (Color recognizer). As shown in Fig. 5b and Fig. S16b, the red values of the RGB color continuously increase until it reaches a maximum plateau. Particularly, the red values have a good linear relationship ($R^2$ = 0.990) with the Cys concentration in the range of 0.1-1 mM. These results demonstrate the feasibility and sensitivity for quantitative detection of biothiols with **DNBS-HCA** on indicator papers.

*3.8. Cytotoxicity and fluorescent imaging in living cells*

The cytotoxicity of the probe **DNBS-HCA** on living cells was tested by the CCK-8 assay. A549 cells were used and incubated with different concentrations of probe (0-16 μM) for 24 h. As shown in Fig. 6, the cell viability is greater than 95%, even

when the cells were incubated with probe **DNBS-HCA** (16 μM) for 24 h. It indicates the low cytotoxicity of the probe on A549 cells.

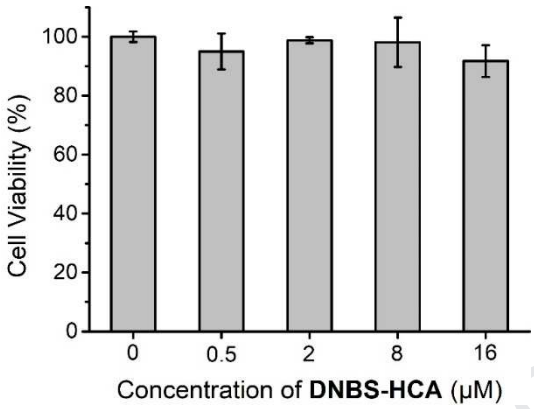


**Fig. 6.** The cell viability of **DNBS-HCA** on A549 cells for 24 h with CCK-8 assay.

Finally, we examined the capability of **DNBS-HCA** to visualize endogenous biothiols in living cells. The fluorescence imaging of A549 cells stained with probe **DNBS-HCA** for 30 min is shown in Fig. S17, the strong fluorescence in the red channel (560-700 nm) and weak fluorescence in the green channel (500-560 nm) can be observed. The red fluorescence should be attributed to the aggregation state of **HCA** molecule produced from the reaction between **DNBS-HCA** and biothiols in cells.

In addition, the results described above demonstrate that the increase of water volume will decrease the reaction rate. This result seems inconsistent with the rapid fluorescence response in living cells, which is totally a water environment. We conjecture that is related to the cellular contents such as proteins. The bovine serum albumin (BSA) in solutions was used to verify this hypothesis. As shown in Fig. S18a, the fluorescence of probe **DNBS-HCA** (40 μM) is almost no changes even with excess Cys (10 eq) or BSA (1mg/mL) in pure water, respectively. However, the

fluorescence shows remarkable enhancement with Cys (10 eq) in BSA (1mg/mL) solution. The reason should be attributed to the promotion of the dispersity of the probe in aqueous solution with the proteins. The biothiol-sensing dynamic curves in BSA solutions were also measured (Fig. S18b). The increase of BSA concentration from 1 to 10 mg/mL will facilitates the reaction rate. So the rapid fluorescence response in living cells is reasonable.

In order to validate the red fluorescence in living cells comes from the biothiols induced probe response, control experiments of cells pretreated with thiol scavenger were used to carry out the fluorescence imaging. In Fig. 7, PC3 cells and A549 cells stained with the probe show remarkable fluorescence. In contrast, the cells pretreated with the thiol scavenger NEM (0.5 mM for 30 min) show weak fluorescence. When the biothiols in living cells are eliminated by the scavenger NEM, no more biothiols can react with the probe **DNBS-HCA** to produce the fluorescent **HCA**. Meanwhile, the fluorescence in blank control without probe is very weak (Fig. S19a, f). The effect of NEM concentration on biothiol imaging was also studied with two different concentrations (0.1 and 0.5 mM). The results indicate that the fluorescence is decreased with the increasing of NEM concentration (Fig. S19b-d, and f). In addition, cells pretreated with NEM were further incubated with Cys to use as a positive control. A significant increase of fluorescence was obtained with the addition of Cys (Fig. S19e, f). These results demonstrate the availability and specificity of **DNBS-HCA** for biothiols detection in living cells.

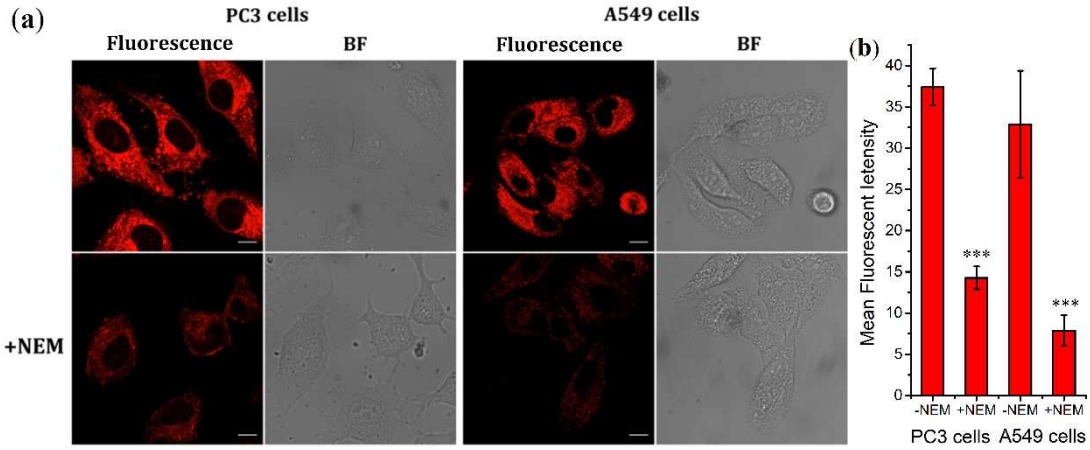


**Fig. 7.** (a) Fluorescent imaging of biothiols in living cells with probe **DNBS-HCA** in red channel. The second row: Cells pretreated with NEM (0.5 mM). BF: bright field imaging. $\lambda_{ex}$ = 488 nm, $\lambda_{em}$ = 560-700 nm. Scale bar = 10 μm. (b) The average fluorescent intensity in cells. Error bars represent standard deviation. Significance was determined using the T test (***, $P < 0.001$).

## 4. Conclusion

In summary, we have developed a novel turn-on fluorescent probe **DNBS-HCA** for biothiols detection based on the 2′-Hydroxychalcone (**HCA**) fluorophore possessing an ESIPT coupled AIE characteristic. The biothiols reactive 2,4-dinitrobenzenesulfonyl (DNBS) moiety of the probe **DNBS-HCA** is employed to block the ESIPT process and quench the fluorescence through PET process. The response reaction of probe **DNBS-HCA** with biothiols will produce the **HCA** fluorophore with large Stokes shift (140 nm) and long-wavelength red fluorescence emission. The probe reveals remarkable fluorescence enhancement of 51- to 94-folds and fast response time of 3 to 15 mins with different biothiols. The biothiols in solution and living cells can be conveniently detected with the probe **DNBS-HCA** due to its excellent properties such as simple synthetic procedure, low cytotoxicity, good sensitivity and high selectivity. In addition, the AIE characteristic of the **HCA** product

also provides strategy for biothiols detection on indicator papers with RGB color red values, which can be handily obtained by smartphone application.

**Acknowledgements**

This work is supported by National Natural Science Foundation of China (21708023), China Postdoctoral Science Foundation (2019M653851XB), Natural Science Basic Research Plan in Shaanxi Province of China (2019JQ-061, 2019JQ-789).

**References**

[1] Filomeni G, Rotilio G, Ciriolo MR. Cell signalling and the glutathione redox system. Biochemical Pharmacology. 2002;64(5-6):1057-64.

[2] Tsunoda S, Avezov E, Zyryanova A, Konno T, Mendes-Silva L, Melo EP, et al. Intact protein folding in the glutathione-depleted endoplasmic reticulum implicates alternative protein thiol reductants. Elife. 2014;3:e03421.

[3] Townsend DM, Tew KD, Tapiero H. The importance of glutathione in human disease. Biomedicine & Pharmacotherapy. 2003;57(3-4):145-55.

[4] Balendiran GK, Dabur R, Fraser D. The role of glutathione in cancer. Cell Biochemistry and Function. 2004;22(6):343-52.

[5] Martin HL, Teismann P. Glutathione-a review on its role and significance in Parkinson's disease. Faseb Journal. 2009;23(10):3263-72.

[6] Chen X, Zhou Y, Peng X, Yoon J. Fluorescent and colorimetric probes for detection of thiols. Chemical Society reviews. 2010;39(6):2120-35.

[7] Yin C, Huo F, Zhang J, Martinez-Manez R, Yang Y, Lv H, et al. Thiol-addition reactions and their applications in thiol recognition. Chemical Society reviews. 2013;42(14):6032-59.

[8] Niu LY, Chen YZ, Zheng HR, Wu LZ, Tung CH, Yang QZ. Design strategies of fluorescent probes for selective detection among biothiols. Chemical Society reviews. 2015;44(17):6143-60.

[9] Yin C-X, Xiong K-M, Huo F-J, Salamanca JC, Strongin RM. Fluorescent probes with multiple binding sites for the discrimination of Cys, Hcy, and GSH. Angewandte Chemie International Edition. 2017;56(43):13188-98.

[10] Lee S, Li J, Zhou X, Yin J, Yoon J. Recent progress on the development of glutathione (GSH) selective fluorescent and colorimetric probes. Coordination Chemistry Reviews. 2018;366:29-68.

[11] Zhou J, Xu S, Dong X, Zhao W, Zhu Q. 3,5-dinitropyridin-2-yl as a fast thiol-responsive capping moiety in the development of fluorescent probes of biothiols. Dyes and Pigments. 2019;167:157-63.

[12] Cao J, Jiang X, Fu N. A sensitive fluorescent probe for imaging biothiol in zebrafish. Dyes and Pigments. 2020;174:107978.

[13] Dai J, Ma C, Zhang P, Fu Y, Shen B. Recent progress in the development of fluorescent probes for detection of biothiols. Dyes and Pigments. 2020;177:108321.

[14] Hong Y, Lam JWY, Tang BZ. Aggregation-induced emission. Chemical Society reviews. 2011;40(11):5361-88.

[15] Luo J, Xie Z, Lam JW, Cheng L, Chen H, Qiu C, et al. Aggregation-induced emission of 1-methyl-1,2,3,4,5-pentaphenylsilole. Chemical Communications. 2001;37(18):1740-1.

[16] Mei J, Leung NLC, Kwok RTK, Lam JWY, Tang BZ. Aggregation-induced emission: Together we shine, united we soar! Chemical Reviews. 2015;115(21):11718-940.

[17] Peng L, Zhou Z, Wei R, Li K, Song P, Tong A. A fluorescent probe for thiols based on aggregation-induced emission and its application in live-cell imaging. Dyes and Pigments. 2014;108:24-31.

[18] Lou X, Hong Y, Chen S, Leung CW, Zhao N, Situ B, et al. A selective glutathione probe based on AIE fluorogen and its application in enzymatic activity assay. Scientific reports. 2014;4:4272.

[19] Cui L, Baek Y, Lee S, Kwon N, Yoon J. An AIE and ESIPT based kinetically resolved fluorescent probe for biothiols. Journal of Materials Chemistry C. 2016;4(14):2909-14.

[20] Chen Q, Jia C, Zhang Y, Du W, Wang Y, Huang Y, et al. A novel fluorophore based on the coupling of AIE and ESIPT mechanisms and its application in biothiol imaging. Journal of Materials Chemistry B. 2017;5(37):7736-42.

[21] Ding S, Liu M, Hong Y. Biothiol-specific fluorescent probes with aggregation-induced emission characteristics. Science China Chemistry. 2018;61(8):882-91.

[22] Li R, Huang X, Lu G, Feng C. A fluorescence and UV/vis absorption dual-signaling probe with aggregation-induced emission characteristics for

specific detection of cysteine. RSC Advances. 2018;8(43):24346-54.

[23] Song H, Zhou Y, Qu H, Xu C, Wang X, Liu X, et al. A novel AIE Plus ESIPT fluorescent probe with a large Stokes shift for cysteine and homocysteine: Application in cell imaging and portable kit. Industrial & Engineering Chemistry Research. 2018;57(44):15216-23.

[24] Gu Y, Zhao Z, Niu G, Zhang R, Zhang H, Shan G-G, et al. Ratiometric detection of mitochondrial thiol with a two-photon active AIEgen. ACS Applied Bio Materials. 2019;2(7):3120-7.

[25] Zhuang C, Zhang W, Sheng C, Zhang W, Xing C, Miao Z. Chalcone: A privileged structure in medicinal chemistry. Chemical Reviews. 2017;117(12):7762-810.

[26] Song Z, Kwok RTK, Zhao E, He Z, Hong Y, Lam JWY, et al. A ratiometric fluorescent probe based on ESIPT and AIE processes for alkaline phosphatase activity assay and visualization in living cells. ACS Applied Materials & Interfaces. 2014;6(19):17245-54.

[27] Jin X, Dong L, Di X, Huang H, Liu J, Sun X, et al. NIR luminescence for the detection of latent fingerprints based on ESIPT and AIE processes. RSC Advances. 2015;5(106):87306-10.

[28] Cheng X, Wang K, Huang S, Zhang H, Zhang H, Wang Y. Organic crystals with near-infrared amplified spontaneous emissions based on 2'-hydroxychalcone derivatives: Subtle structure modification but great property change. Angewandte Chemie International Edition. 2015;54(29):8369-73.

[29] Zahid NI, Mahmood MS, Subramanian B, Mohd. Said S, Abou-Zied OK. New insight into the origin of the red/near-infrared intense fluorescence of a crystalline 2-hydroxychalcone derivative: A comprehensive picture from the excited-state femtosecond dynamics. Journal of Physical Chemistry Letters. 2017;8(22):5603-8.

[30] Dommett M, Rivera M, Crespo-Otero R. How inter- and intramolecular processes dictate aggregation-induced emission in crystals undergoing excited-state proton transfer. Journal of Physical Chemistry Letters.

2017;8(24):6148-53.

[31] Luo Z, Lv T, Zhu K, Li Y, Wang L, Gooding JJ, et al. Paper-based ratiometric fluorescence analytical devices towards point-of-care testing of human serum albumin. Angewandte Chemie International Edition. 2020;59(8):3131-6.

[32] Luo Z, Liu B, Qin T, Zhu K, Zhao C, Pan C, et al. Cyclization of chalcone enables ratiometric fluorescence determination of hydrazine with a high selectivity. Sensors and Actuators B: Chemical. 2018;263:229-36.

[33] Luo Z, Liu B, Zhu K, Huang Y, Pan C, Wang B, et al. An environment-sensitive fluorescent probe for quantification of human serum albumin: Design, sensing mechanism, and its application in clinical diagnosis of hypoalbuminemia. Dyes and Pigments. 2018;152:60-6.

[34] Zhu K, Qin T, Zhao C, Luo Z, Huang Y, Liu B, et al. A novel fluorescent turn-on probe for highly selective detection of nitroreductase in tumor cells. Sensors and Actuators B: Chemical. 2018;276:397-403.

[35] Li R, Yan L, Wang Z, Qi Z. An aggregation-induced emissive NIR luminescent based on ESIPT and TICT mechanisms and its application to the detection of Cys. Journal of Molecular Structure. 2017;1136:1-6.

[36] Han C, Song B, Liang X, Pan H, Dong W. Design and application of a fluorescent probe based on ESIPT mechanism for the detection of Cys with o-hydroxyacetophenone structure. Analytical Methods. 2019;11(19):2513-7.

[37] Maeda H, Matsuno H, Ushida M, Katayama K, Saeki K, Itoh N. 2,4-Dinitrobenzenesulfonyl fluoresceins as fluorescent alternatives to ellman's reagent in thiol-quantification enzyme assays. Angewandte Chemie International Edition. 2005;44(19):2922-5.

[38] Lan M, Wu J, Liu W, Zhang H, Zhang W, Zhuang X, et al. Highly sensitive fluorescent probe for thiols based on combination of PET and ESIPT mechanisms. Sensors and Actuators B-Chemical. 2011;156(1):332-7.

[39] Lu J, Song Y, Shi W, Li X, Ma H. A long-wavelength fluorescent probe for imaging reduced glutathione in live cells. Sensors and Actuators B-Chemical. 2012;161(1):615-20.

[40] Li M, Wu X, Wang Y, Li Y, Zhu W, James TD. A near-infrared colorimetric fluorescent chemodosimeter for the detection of glutathione in living cells. Chemical Communications. 2014;50(14):1751-3.

[41] Liu H-W, Zhang X-B, Zhang J, Wang Q-Q, Hu X-X, Wang P, et al. Efficient two-photon fluorescent probe with red emission for imaging of thiophenols in living cells and tissues. Analytical Chemistry. 2015;87(17):8896-903.

[42] Liu K, Shang H, Kong X, Lin W. A novel near-infrared fluorescent probe with a large Stokes shift for biothiol detection and application in in vitro and in vivo fluorescence imaging. Journal of Materials Chemistry B. 2017;5(21):3836-41.

[43] Wang F-F, Fan X-Y, Liu Y-J, Gao T, Huang R, Jiang F-L, et al. Design, synthesis, cell imaging, kinetics and thermodynamics of reaction-based turn-on fluorescent probes for the detection of biothiols. Dyes and Pigments. 2017;145:451-60.

[44] Chen D, Yang J, Dai J, Lou X, Zhong C, Yu X, et al. A low background D-A-D type fluorescent probe for imaging of biothiols in living cells. Journal of Materials Chemistry B. 2018;6(32):5248-55.

[45] Sedgwick AC, Gardiner JE, Kim G, Yevglevskis M, Lloyd MD, Jenkins ATA, et al. Long-wavelength TCF-based fluorescence probes for the detection and intracellular imaging of biological thiols. Chemical Communications. 2018;54(38):4786-9.

[46] Wang F-F, Liu Y-J, Wang B-B, Gao L-X, Jiang F-L, Liu Y. A BODIPY-based mitochondria-targeted turn-on fluorescent probe with dual response units for the rapid detection of intracellular biothiols. Dyes and Pigments. 2018;152:29-35.

[47] Wang Y, Wang L, Jiang E, Zhu M, Wang Z, Fan S, et al. A colorimetric and ratiometric dual-site fluorescent probe with 2,4-dinitrobenzenesulfonyl and aldehyde groups for imaging of aminothiols in living cells and zebrafish. Dyes and Pigments. 2018;156:338-47.

[48] Lin X, Hu Y, Yang D, Chen B. Cyanine-coumarin composite NIR dye based instantaneous -response probe for biothiols detection and oxidative stress assessment of mitochondria. Dyes and Pigments. 2020;174:107956.

[49] Teshima T, Takeishi M, Arai T. Red fluorescence from tautomers of

2'-hydroxychalcones induced by intramolecular hydrogen atom transfer. New Journal of Chemistry. 2009;33(6):1393-401.

[50] Wang H, Yang L, Chu S, Liu B, Zhang Q, Zou L, et al. Semiquantitative visual detection of lead ions with a smartphone via a colorimetric paper-based analytical device. Analytical Chemistry. 2019;91(14):9292-9.

[51] Bai Y, An N, Liu C-P, Wang C, Chen D, Liu Y-Z, et al. Facile construction of shape-regulated β-cyclodextrin-based supramolecular self-assemblies for drug delivery. Carbohydrate Polymers. 2020;231:115714.

**Highlights:**

- An ESIPT coupled AIE fluorescent probe was developed for biothiols detection.
- The fluorescence of 2′-Hydroxychalcone is quenched by a biothiols-reactive moiety.
- The excellent fluorescent response properties indicates the availability in cells.
- The biothiols was also conveniently detected with the probe on indicator papers.

**Declaration of interests**

☒ The authors declare that they have no known competing financial interests or personal relationships that could have appeared to influence the work reported in this paper.

☐The authors declare the following financial interests/personal relationships which may be considered as potential competing interests: